Letter

Nonlinear Hall effect of magnetized two-dimensional spin-$\frac{3}{2}$ heavy holes

Sina Gholizadeh ,[1,2] James H. Cullen,[1] and Dimitrie Culcer[1,2]
[1]*School of Physics, The University of New South Wales, Sydney 2052, Australia*
[2]*ARC Centre of Excellence in Future Low-Energy Electronics Technologies, The University of New South Wales, Sydney 2052, Australia*

(Received 4 July 2022; revised 19 December 2022; accepted 31 December 2022; published 17 January 2023)

We identify a sizable nonlinear Hall effect of spin-3/2 heavy holes in zincblende nanostructures, driven by a quadrupole interaction with the electric field formerly believed to be negligible. The interaction is enabled by T_d-symmetry, reflects inversion breaking, and in two dimensions results in an electric-field correction to the in-plane g factor. The effect can be observed in state-of-the-art heterostructures, either via magnetic doping or by using a vector magnet, where even for small perpendicular magnetic fields it is comparable in magnitude to topological materials.

DOI: 10.1103/PhysRevB.107.L041301

Introduction. Recent years have seen a surge in interest in nonlinear electromagnetic responses motivated by outstanding advances in topological materials and semiconductor growth [1–5]. Nonlinear optical responses such as second-harmonic generation [6–9], shift currents [10–12], the circular photogalvanic [13], and resonant photovoltaic effects [14] are being explored for technological applications including AC to DC conversion, photo-detection, and energy harvesting. At the same time, nonlinear electrical responses have revealed the existence of novel physical phenomena such as the anomalous Hall effect in time-reversal preserving systems [15], which was recently observed in topological materials [16–18].

Second-order electrical responses require inversion symmetry breaking [19–22]. Aside from most topological materials, which have been at the heart of this effort, tetrahedral semiconductors likewise break inversion symmetry. This symmetry breaking is strong in zincblende crystals such as GaAs, and is associated with the spin-orbit interaction, which is particularly large in spin-3/2 hole systems. The effective spin-3/2 makes holes qualitatively different from spin-1/2 electrons [23–40], endowing them with unconventional properties such as a density dependent in-plane g factor [41,42], a strong anisotropy in both of the longitudinal conductivity and the Hall coefficient R_H [43,44], a nonmonotonic Rashba spin-orbit coupling [45], a planar anomalous Hall effect [46], and superconductivity [47]. Until recently tetrahedral T_d symmetry terms were believed to be negligible in hole systems [25], yet a more careful evaluation has demonstrated their size to be significant [48], so that sizable second-order electrical responses should be possible in hole systems.

In this work, we show that tetrahedral symmetry terms lead to a nonlinear Hall effect in a symmetric hole quantum well (QW). The effect occurs in the presence of both in-plane and out-of-plane Zeeman fields, the latter of which can be produced either by a small magnetic field or by magnetic impurities in a ferromagnetic semiconductor. The role of the T_d terms can be understood as an electric field induced shear term in the in-plane g factor. Our main result is summarized in Figs. 1 and 2. We find a sizable nonlinear Hall current density along the y axis, accompanied by a much smaller nonlinear longitudinal current density, not shown. The effect can be easily measured in readily available hole nanostructures, which provide a straightforward setup for probing the existence of tetrahedral-symmetry terms. Based on realistic parameters we find that the nonlinear Hall effect in spin-3/2 holes can be comparable in magnitude to the values reported recently in topological materials [18]. Aside from the novelty of identifying a nonlinear electrical response purely due to holes, as opposed to well-known optical transitions linking the valence and conduction bands, a sizable tetrahedral contribution beyond the Luttinger model will have important repercussions for hole-based quantum computing [47,49–65], enabling strategies for the electrical manipulation of holes.

Hamiltonian. We consider a symmetric hole quantum well grown in a zincblende heterostructure along the high-symmetry crystallographic direction (001). The confinement is along the z axis. For concreteness we consider GaAs with Luttinger parameters for $\gamma_1 = 6.85$, $\gamma_2 = 2.10$, and $\gamma_3 = 2.90$ [25], and work in the axial approximation, where $\bar{\gamma} = (\gamma_2 + \gamma_3)/2$. The total Hamiltonian $H = H_0 + U + H_E$ includes the band Hamiltonian, the disorder potential, and the applied electric field. The band Hamiltonian $H_0 = \hbar^2 k^2/2m^* + H_Z$ where $m^* = m_0/(\gamma_1 + \bar{\gamma})$ is the in-plane effective mass, m_0 is the bare electron mass, and H_Z is given b y [25,41,66],

$$H_Z = \Delta_1 B_+ k_+^2 \sigma_- + \Delta_2 B_- k_+^4 \sigma_- + \text{H.c.} + M\sigma_3, \qquad (1)$$

where Δ_1 and Δ_2 are the g factors, $B_\pm = B_x \pm iB_y$ represent the in-plane magnetic field of magnitude $B_\parallel$, H.c. is Hermitian conjugate, $k_\pm = k_x \pm ik_y$, while $\sigma_\pm = (1/2)(\sigma_x \pm i\sigma_y)$. Without loss of generality we set $B_\parallel = B_x$. We have denoted the Zeeman field in the $\hat{z}$ direction by M, and define it so that M has units of energy. The eigenvalues of H_0 are $\epsilon_{\boldsymbol{k}}^{(\pm)} = \epsilon_k^{(0)} \pm \Omega_{\boldsymbol{k}}$ where $\epsilon_k^{(0)} = \hbar^2 k^2/2m^*$ is kinetic

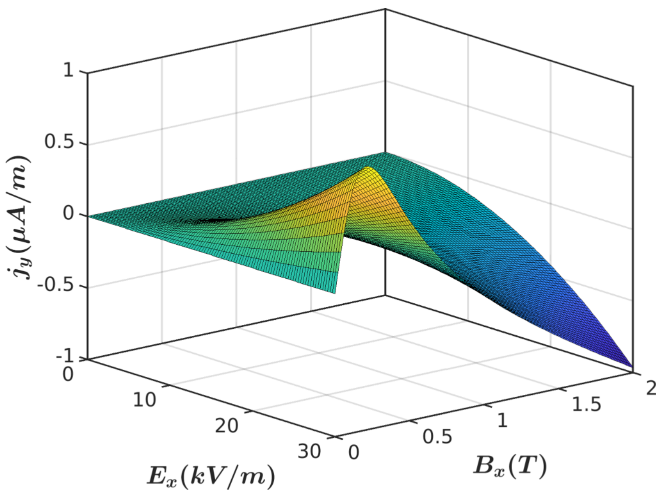

FIG. 1. Nonlinear Hall current density $\parallel \hat{\boldsymbol{y}}$ as a function of the in-plane magnetic field and driving electric field for a 30 nm GaAs QW with M = 0.1 meV, $\Delta_1 = -1 \times 10^{-17}$ meV m^2 T^{-1}, and $\Delta_2 = 2 \times 10^{-33}$ meV m^4 T^{-1} [41].

part and energy dispersion is split by $\Omega_{\boldsymbol{k}} = \sqrt{M^2 + B_\parallel^2 k^4 G_{\boldsymbol{k}}}$, and $G_{\boldsymbol{k}} = (\Delta_1)^2 + k^4(\Delta_2)^2 + 2k^2\Delta_1\Delta_2\cos(2\theta)$. The term $\propto B_\parallel k^2$ has been known [25], while recent work has identified an additional term $\propto B_\parallel k^4$ [41] which has been confirmed experimentally [66]. The prefactors Δ_1 and Δ_2 are functions of k and decrease strongly at larger wave vectors [41,66]. In our work we evaluate the coefficients for the specific carrier density we have chosen. For a symmetric QW there is no Rashba spin-orbit interaction [25,67,68]. Likewise, we have not included the Dresselhaus interaction in the Hamiltonian H_0 because it does not contribute to the nonlinear signal: we have verified this explicitly. The interaction with a uniform electric field $\boldsymbol{E}$ makes two contributions to H_E, namely $H_E = e\boldsymbol{E}.\hat{\boldsymbol{r}} + H_\lambda$. The first is the electrostatic potential, while the second arises from T_d symmetry, and, as shown in the Supplemental Material [69], has the form

$$H_\lambda = ie\lambda M(E_+k_-^2\sigma_+ - E_-k_+^2\sigma_-), \tag{2}$$

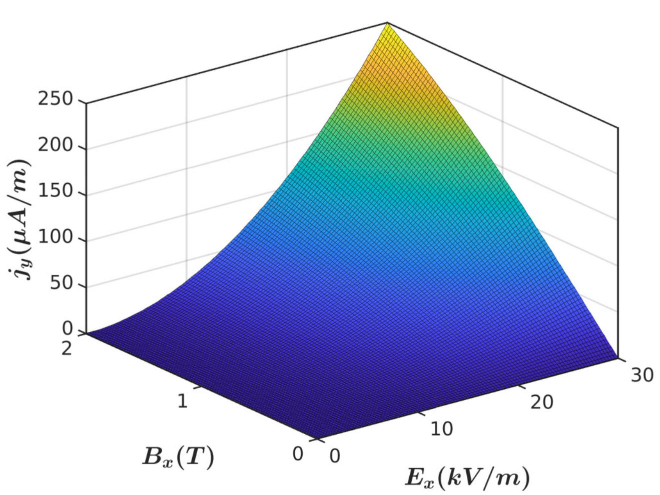

FIG. 2. Nonlinear Hall current density $\parallel \hat{\boldsymbol{y}}$ as a function of the in-plane magnetic field and driving electric field for a 30 nm GaAs QW (M = 2 meV, other parameters as in Fig. 1.)

in which $E_\pm$ is the in-plane electric field, M is the out-of-plane Zeeman field which we take to have units of energy, and λ is a material-specific parameter whose magnitude will be determined below. We transform H_λ to the eigenstate basis of H_0. Without loss of generality we take $\boldsymbol{E} \parallel \hat{\boldsymbol{x}}$, yielding $\tilde{H}_\lambda = eE_xk^2M\lambda\tilde{\sigma}_y$, where the tilde indicates matrices in the eigenstate basis. H_λ can be understood as an electric-field correction to the Zeeman Hamiltonian mediated by the T_d-symmetry terms. Thus the nonlinear response we discuss is traced to a new interaction with the electric field, and has no equivalent in any studied previously, e.g., it is not related to the Berry curvature dipole of Ref. [15].

Kinetic equation. To first order in $\boldsymbol{E}$ we have [70]

$$\frac{\partial \rho_E}{\partial t} + \frac{i}{\hbar}[H_0, \langle\rho_E\rangle] + J(\langle\rho_E\rangle) = -\frac{i}{\hbar}[H_E, \langle\rho_0\rangle], \tag{3}$$

where ρ_0 and ρ_E are the equilibrium and first-order density matrices, respectively. The scattering term in the Born approximation $J(\langle\rho\rangle) = \frac{1}{\hbar^2}\int_0^\infty dt'\langle[U, [e^{-iH_0t'/\hbar}U\,e^{iH_0t'/\hbar}, \langle\rho(t)\rangle]]\rangle$, with a short-range disorder $U(\boldsymbol{r}) = U_0\sum_i \delta(\boldsymbol{r} - \boldsymbol{r}_i)$, and $\langle U(\boldsymbol{r})U(\boldsymbol{r}')\rangle = n_iU_0^2\,\delta(\boldsymbol{r} - \boldsymbol{r}')$ with n_i the impurity density. The disorder potential is responsible for the scattering time τ, introduced below, which keeps the Fermi surface near equilibrium. The driving term has two contributions

$$D_{E\boldsymbol{k}} = \frac{eE_x}{\hbar}\left\{\frac{\partial \rho_0}{\partial k_x} - i[\mathcal{R}_{k_x}, \rho_0]\right\} - \frac{i}{\hbar}[\tilde{H}_\lambda, \rho_0] \tag{4}$$

in which $\mathcal{R}_{k_x} = \langle u_{\boldsymbol{k}}|(i\partial u_{\boldsymbol{k}}/\partial k_x)\rangle$ is the Berry connection. In the crystal momentum representation, i.e., $|m, \boldsymbol{k}\rangle = e^{i\boldsymbol{k}.\boldsymbol{r}}|u_{m\boldsymbol{k}}\rangle$, the equilibrium density matrix is $f_0(\epsilon_{\boldsymbol{k}}^{(m)})\delta^{mm'}$, where f_0 denotes the Fermi-Dirac distribution. The terms in curly brackets are the consequences of $e\boldsymbol{E}\cdot\hat{\boldsymbol{r}}$. The first term in curly bracket is the Fermi surface response. The remaining two are the Fermi sea response.

As shown in Ref. [44] we can account for orbital magnetic field effects by first replacing the driving term in (3) with

$$D_{B\boldsymbol{k}} = \frac{e}{2\hbar}\left\{\boldsymbol{v} \times \boldsymbol{B}, \frac{\partial \rho_E}{\partial \boldsymbol{k}}\right\}, \tag{5}$$

and subsequently taking $\rho_0 \to \rho_E$ and $\rho_E \to \rho_{E,B,}$ where $\rho_{E,B}$ density matrix to first order in both $\boldsymbol{E}$ and $\boldsymbol{B}$. Here $\boldsymbol{v} = \partial H_0/\partial\boldsymbol{k} - i[\boldsymbol{\mathcal{R}}, H_0]$ is the velocity operator. Note that, for an in-plane magnetic field the coupling of orbital terms to higher order states is already included in the Hamiltonian through Δ_1 and Δ_2 [25]. Furthermore, since the system is 2D for an in-plane magnetic field the driving term $D_{B\boldsymbol{k}}$ is trivially zero. However, the orbital effect of an out-of-plane magnetic field, if present, is nontrivial and will produce a correction to our results. Since a full treatment of an out-of-plane magnetic field would require an intensive calculation, it is not considered in detail in our main setup. An estimation of the correction by an out-of-plane field is provided in the Supplemental Material [69].

Second-order electrical response. To determine ρ_E we solve Eq. (3) to linear order in $\boldsymbol{E}$. Then, to find the second-order density matrix ρ_{E2}, we repeat the procedure, substituting $\rho_0 \to \rho_E$ and $\rho_E \to \rho_{E2}$. We analytically derive the conductivity with Δ_2 set to zero. For pedagogical purposes we perform an analytical calculation first, using a simplified model. $G_{\boldsymbol{k}}$ becomes simply Δ_1^2 if we neglect Δ_2. The term

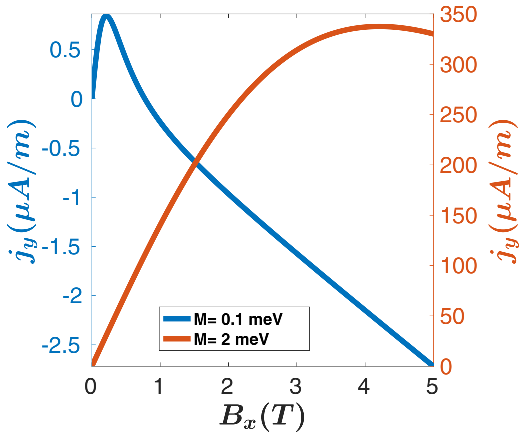

FIG. 3. The nonlinear Hall effect is a nonmonotonic function of the in-plane magnetic field, shown here for two different values of the out-of-plane Zeeman field: $M = 2\,\text{meV}$ and $M = 0.1\,\text{meV}$. The electric field is $E_x = 30\,\text{kV/m}$.

$\Omega_{\boldsymbol{k}}$ is function of both k and θ if we take into account both g factors. But if we only consider Δ_1, the dispersion is isotropic. To second order in the electric field $j_x = \chi_{xxx}E_x^2$ and $j_y = \chi_{yxx}E_x^2$, where

$$\chi_{xxx} = \frac{2e^3B_x^3\Delta_1^3k_F^6mM^2\lambda}{\pi\hbar^3\Omega_F^4},$$
$$\chi_{yxx} = \frac{2e^3\lambda mM\tau B_x\Delta_1k_F^2\left(\Omega_F^2+M^2\right)}{\pi\hbar^4\Omega_F^2}, \tag{6}$$

where $\Omega_F = \sqrt{M^2 + B_x^2\Delta_1^2k_F^4}$, k_F is the Fermi wave vector, and the momentum relaxation time $\tau = \hbar^3/(n_iU^2m)$. Numerically we extend our results for the general case where Δ_2 is taken into account. The transverse nonlinear current density, shown in Figs. 1–4, is larger than its longitudinal counterpart (not shown) by several orders of magnitude. In both cases, in the presence of Δ_2, the behavior of the current density is nonmonotonic in terms of the magnetic field, but in general $|j_y|$ increases linearly in terms of the magnetic field while the magnetic field is larger compared to magnetization. As we expect, the current density in second order behaves as an increasing parabolic function in terms of electric field (Figs. 1 and 2). In Fig. 4 we can see that in the range of values set for magnetic and electric fields, the current density behaves almost linearly as a function of magnetization. On the other hand, in Fig. 3 the change in the direction of the current reflects a competition between the in-plane Zeeman terms when Δ_1 and Δ_2 are both present. Whereas the contributions $\propto \Delta_1^2$, Δ_2^2 have the same sign, the contribution $\propto \Delta_1\Delta_2$ has the opposite sign, and depends on M. While there is no analytical expression for this case, the overall shape is the same: for $M = 2$ meV the current will likewise reach a maximum and then decrease, only this decrease will occur at much larger values of $B_\parallel$. For comparison we have provided a version of Figs. 1–3 without Δ_2 in the Supplemental Material [69].

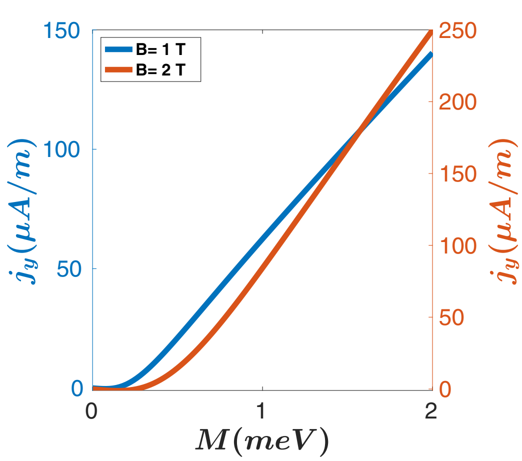

FIG. 4. The nonlinear Hall current is approximately linear in the magnetization M. Here $E_x = 30$ kV/m.

To obtain λ we apply the Schrieffer-Wolff transformation to the Luttinger Hamiltonian combined with the electric dipole and Zeeman Hamiltonians to project the system to the HH subspace [69], finding $\lambda = (3a_B\xi)/(8\bar{\gamma}\langle k_z^2\rangle^2\mu)$, in which a_B is the Bohr radius, and ξ controls the strength of electric-dipole terms. For the following values, $\xi = 0.2$, $\mu = \hbar^2/m_0$, $\bar{\gamma} = 2.5$, $k_z = (\pi/30\,\text{nm})$, we obtain $\lambda = 1.08 \times 10^{-6}\ \text{ms}^2\text{kg}^{-1}$. The size of H_λ may be quantified as $e\lambda Mk_F^2E$, while the electrostatic potential is $\approx eE/k_F$. The ratio of the two is λMk_F^3. Estimating $M \approx 1$ meV and $k_F \approx 10^8\ \text{m}^{-1}$, the ratio is 10^{-4}. In a realistic 2D semiconductor k_F is never above $5 \times 10^8\ \text{m}^{-1}$, yielding a ratio of 10^{-2}.

Discussion. The second-order response is directly proportional to λ, and our expression for λ is proportional to the size of the QW. Therefore, we expect this effect will be pronounced in larger wells, thus the effect will be stronger in, e.g., a 30 nm well than in a 10 nm well. However, here λ is derived using a SW transformation to leading order in perturbation theory, its accuracy depends on the energy gap between the lowest heavy hole and light hole subbands. As the confinement becomes weaker the perturbation theory will have to be extended to second and then higher orders, at which point we no longer expect the trend we find here to apply. Naturally, as the well becomes wider at around 60 nm, perturbation theory becomes inapplicable altogether.

It is easy to see that the second-order response is thoroughly dependent on ξ, meaning that at $\xi = 0$ (for crystals with a center of inversion symmetry) the second-order response vanishes. Marcellina *et al.* [44] shows that in spin-3/2 system with two different g factors (each have different winding numbers), there appears a sizable anisotropy in conductivities and Hall coefficients. We have shown that in the similar system a sizable nonlinear response can be probed using H_λ [Eq. (2)]. Note that, although the nonlinear Hall effect is stronger in higher mobility systems, the ratio $j^{(2)}/\sigma_{xx}$ is independent of the mobility, playing the role of a nonlinear Hall coefficient.

In the absence of Δ_2 the absolute value of the current density increases monotonically as a function of the out-of-plane Zeeman energy and in-plane magnetic field. When either quantity, i.e., M or B_x, dominates, $|j_y|$ becomes linear in that

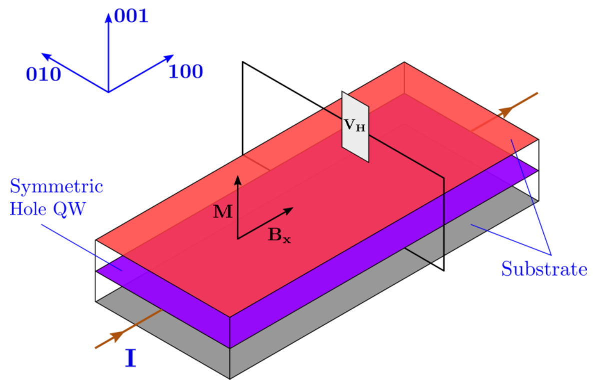

FIG. 5. Schematic of one potential experimental setup. The effect can be detected by measuring the Hall voltage.

quantity. On the other hand, when Δ_2, which has a different sign from Δ_1, is accounted for in the Hamiltonian, $|j_y|$ is nonmonotonic as a function of B_x in the range of $M(\text{meV}) \in [0, 2]$ but it still behaves monotonically as a function of M in the range of $B_x(T) \in [0, 2]$. Nevertheless, the current density behaves linearly at comparatively large (small) values of M and small (large) values of B_x. One can also see from Fig. 3 that the first derivative of j_y changes signs depending on the size of the magnetization.

Experimental observation. There is considerable flexibility in regard to experimental observation, with one possibility illustrated in Fig. 5. One requires a low-frequency alternating field, which can be generated by an oscillator with a frequency of the order of $\omega/(2\pi) \sim 100$ Hz. The Hall voltage at 2ω can then be read out. In general $\omega\tau \ll 1$, hence our DC calculation is appropriate. The perpendicular Zeeman field can be attained either via a magnetic doping, as in ferromagnetic semiconductors, or by applying a perpendicular magnetic field. We discuss each in turn. To facilitate comparison with topological materials we use the sample size in Ref. [18].

The easiest way is using an unmagnetized GaAs sample together with a vector magnet generating an arbitrary magnetic field. The out-of-plane magnetic field can be set so that the Zeeman energy is $M \approx 0.1$ meV. To determine the Hall voltage we start with the relationship between the resistivity and conductivity tensors

$$\begin{pmatrix} \rho_{xx} & \rho_{xy} \\ \rho_{yx} & \rho_{yy} \end{pmatrix} = \frac{1}{\sigma_{xx}^2 + \sigma_{yx}^2} \begin{pmatrix} \sigma_{xx} & -\sigma_{xy} \\ \sigma_{xy} & \sigma_{xx} \end{pmatrix}. \tag{7}$$

The induced nonlinear Hall electric field takes the form

$$E_y^{(2)} \approx \frac{\chi_{yxx}}{\sigma_{xx}} E_x^2, \tag{8}$$

as outlined in the Supplemental Material [69]. Assuming $M = 0.1$ meV, using Fig. 1 we take the current density $0.96\,\mu\text{A/m}$ corresponding to the magnetic field, electric field, and magnetization provided at $B_x = 2\,T$, $E_x = 30$ kV/m, and $M = 0.1$ meV. To find the conductivity we consider a relaxation time $\tau = 1$ ps. The hole carrier density is taken to be $1.86 \times 10^{15}\,m^{-2}$. The heavy hole in-plane mass is $m^* = m_0/(\gamma_1 + \bar{\gamma})$, yielding

$$\sigma_{xx} = \frac{ne^2\tau}{m^*} \approx 12.7\,\frac{e^2}{h}, \tag{9}$$

hence the induced nonlinear Hall electric field $E_y^{(2)} \approx 2 \times 10^{-3}$ V/m and a corresponding nonlinear Hall voltage $V_y^{(2)} = E_y^{(2)} d = 18$ nV.

A class of state-of-art samples that can be used to study nonlinear effects are magnetic semiconductors, such as GaMnAs [71–78]. The magnetization easy axis in GaMnAs can be either in the plane or out of the plane [79], and the orientation can be tailored by means of strain. We focus on the latter case in this example and assume a larger value of $M \approx 2$ meV. From Fig. 2 we take the current density to be 0.25 mA/m, corresponding to a magnetic field and electric field of $B_x = 2\,T$ and E = 30 kV/m, respectively. Using the same carrier density and relaxation time as above we find the same value for σ_{xx}, whereupon the induced nonlinear Hall electric field $E_y^{(2)} \approx 0.5$ V/m, and, in a sample of width 9.2 µm as in [18], we find a Hall voltage $V_y^{(2)} \approx 5\,\mu$V, which is comparable in size to Ref. [18].

The effect depends to some extent on the QW shape due to the difference in confinement energies. The physics is driven by the coupling between the lowest heavy-hole and light-hole sub-bands, HH1 and LH1. For a square well the HH1-LH1 splitting is $2\bar{\gamma}\hbar^2\pi^2/(m_0 d^2)$. In a parabolic well ranging from $-d/2$ to $d/2$, the HH1-LH1 splitting is $8\gamma\hbar^2/(m_0 d^2)$. Thus one expects the effect to be larger in a parabolic well than in a square well of equivalent width. Based on Eq. (5), the effect will be 2.5 times larger both at large M and small M.

For the main calculation, orbital effects of an out-of-plane magnetic field were not considered. We have carried out a simple approximation of the corrections from an out-of-plane magnetic field in which we used a scattering time approximation ($J(\rho_E) = \frac{\rho_E}{\tau}$) and simplified the Hamiltonian by setting $\Delta_2 = 0$. We find that an out-of plane magnetic field can give rise to significant corrections both to the second order longitudinal and Hall currents. The corrections are at lowest order $\propto B^2$, the nonlinear Hall current correction will be negligible for out-of-plane magnetic fields on the order of 100 mT and will become significant for larger fields. For a system with both in-plane and out-of-plane fields of 1T, we find the correction enhances or suppresses the nonlinear Hall current by ≈50% depending on the field's orientation. Importantly, even with these corrections the nonlinear Hall effect still remains entirely dependent on the Zeeman and quadrupole terms, since the Hamiltonian does not break inversion symmetry.

Summary. We have shown that in a symmetric quasi-2D hole system a sizable nonlinear Hall effect is present, driven by tetrahedral symmetry terms that go beyond the Luttinger model. The effect is measurable either in a conventional GaAs sample using a vector magnet, or in a sample of ferromagnetic GaAs in a magnetic field, where the magnetic field orientation is chosen depending on the direction of the magnetization. The effect can be as strong in semiconductors as in topological materials suggesting that spin-3/2 hole systems are ideal candidates for observing nonlinear electromagnetic responses, in particular since their mobilities are typically orders of magnitude larger than those of topological materials.

Acknowledgments. This work is supported by the Australian Research Council Centre of Excellence in Future Low-Energy Electronics Technologies (Project No. CE170100039). This project was supported by an Australian Government Research Training Program (RTP) Scholarship.

[1] R. W. Boyd, *Nonlinear Optics* (Academic, 2020).

[2] T. Morimoto and N. Nagaosa, Sci. Adv. **2**, e1501524 (2016).

[3] H. Watanabe and Y. Yanase, Phys. Rev. X **11**, 011001 (2021).

[4] D. Culcer, A. C. Keser, Y. Li, and G. Tkachov, 2D Mater. **7**, 022007 (2020).

[5] E. Dobardžić, M. Dimitrijević, and M. V. Milovanović, Phys. Rev. B **91**, 125424 (2015).

[6] F. Hipolito and V. M. Pereira, 2D Mater. **4**, 021027 (2017).

[7] L. E. Golub and S. A. Tarasenko, Phys. Rev. B **90**, 201402(R) (2014).

[8] L. E. Golub, S. A. Tarasenko, M. V. Entin, and L. I. Magarill, Phys. Rev. B **84**, 195408 (2011).

[9] Y. Gao and F. Zhang, Phys. Rev. B **103**, L041301 (2021).

[10] J. E. Sipe and A. I. Shkrebtii, Phys. Rev. B **61**, 5337 (2000).

[11] M. Nakamura, S. Horiuchi, F. Kagawa, N. Ogawa, T. Kurumaji, Y. Tokura, and M. Kawasaki, Nat. Commun. **8**, 1 (2017).

[12] T. Rangel, B. M. Fregoso, B. S. Mendoza, T. Morimoto, J. E. Moore, and J. B. Neaton, Phys. Rev. Lett. **119**, 067402 (2017).

[13] Y. Zhang, H. Ishizuka, J. van den Brink, C. Felser, B. Yan, and N. Nagaosa, Phys. Rev. B **97**, 241118(R) (2018).

[14] P. Bhalla, A. H. MacDonald, and D. Culcer, Phys. Rev. Lett. **124**, 087402 (2020).

[15] I. Sodemann and L. Fu, Phys. Rev. Lett. **115**, 216806 (2015).

[16] Z. Z. Du, C. M. Wang, H.-Z. Lu, and X. C. Xie, Phys. Rev. Lett. **121**, 266601 (2018).

[17] Q. Ma, S.-Y. Xu, H. Shen, D. MacNeill, V. Fatemi, T.-R. Chang, A. M. Mier Valdivia, S. Wu, Z. Du, C.-H. Hsu *et al.*, Nature **565**, 337 (2019).

[18] K. Kang, T. Li, E. Sohn, J. Shan, and K. F. Mak, Nat. Mater. **18**, 324 (2019).

[19] L. D. Tzuang, K. Fang, P. Nussenzveig, S. Fan, and M. Lipson, Nat. Photonics **8**, 701 (2014).

[20] Y. Tokura and N. Nagaosa, Nat. Commun. **9**, 3740 (2018).

[21] Y. Gao and D. Xiao, Phys. Rev. Lett. **122**, 227402 (2019).

[22] L. Shao, W. Mao, S. Maity, N. Sinclair, Y. Hu, L. Yang, and M. Lončar, Nat. Electron **3**, 267 (2020).

[23] J. M. Luttinger, Phys. Rev. **102**, 1030 (1956).

[24] W. W. Chow and S. W. Koch, *Semiconductor-Laser Fundamentals: Physics of the Gain Materials* (Springer Science & Business Media, 1999).

[25] R. Winkler, *Spin-Orbit Coupling Effects in Two-Dimensional Electron and Hole Systems*, Vol. 191 (Springer, 2003).

[26] M. Cardona and Y. Y. Peter, *Fundamentals of Semiconductors*, Vol. 619 (Springer, 2005).

[27] R. Winkler, D. Culcer, S. Papadakis, B. Habib, and M. Shayegan, Semicond. Sci. Technol. **23**, 114017 (2008).

[28] C. Wang, S. Liu, Q. Lin, X. Lei, and M. Pang, J. Phys.: Condens. Matter **22**, 095803 (2010).

[29] T. Biswas and T. K. Ghosh, J. Appl. Phys. **115**, 213701 (2014).

[30] A. Mawrie, T. Biswas, and T. K. Ghosh, J. Phys.: Condens. Matter **26**, 405301 (2014).

[31] M. V. Durnev, M. M. Glazov, and E. L. Ivchenko, Phys. Rev. B **89**, 075430 (2014).

[32] K. V. Shanavas, Phys. Rev. B **93**, 045108 (2016).

[33] G. Akhgar, O. Klochan, L. H. Willems van Beveren, M. T. Edmonds, F. Maier, B. J. Spencer, J. C. McCallum, L. Ley, A. R. Hamilton, and C. I. Pakes, Nano Lett. **16**, 3768 (2016).

[34] E. Marcellina, A. R. Hamilton, R. Winkler, and D. Culcer, Phys. Rev. B **95**, 075305 (2017).

[35] A. Mawrie, S. Verma, and T. K. Ghosh, J. Phys.: Condens. Matter **29**, 465303 (2017).

[36] M. Marx, J. Yoneda, Á. G. Rubio, P. Stano, T. Otsuka, K. Takeda, S. Li, Y. Yamaoka, T. Nakajima, A. Noiri *et al.*, arXiv:2003.07079.

[37] K. Wang, G. Xu, F. Gao, H. Liu, R.-L. Ma, X. Zhang, Z. Wang, G. Cao, T. Wang, J.-J. Zhang *et al.*, Nat. Commun. **13**, 206 (2022).

[38] S. Bosco, B. Hetényi, and D. Loss, PRX Quantum **2**, 010348 (2021).

[39] F. N. M. Froning, M. J. Rančić, B. Hetényi, S. Bosco, M. K. Rehmann, A. Li, E. P. A. M. Bakkers, F. A. Zwanenburg, D. Loss, D. M. Zumbühl, and F. R. Braakman, Phys. Rev. Res. **3**, 013081 (2021).

[40] T. Biswas, S. Chowdhury, and T. K. Ghosh, Eur. Phys. J. B **88**, 220 (2015).

[41] D. S. Miserev and O. P. Sushkov, Phys. Rev. B **95**, 085431 (2017).

[42] E. Marcellina, A. Srinivasan, D. S. Miserev, A. F. Croxall, D. A. Ritchie, I. Farrer, O. P. Sushkov, D. Culcer, and A. R. Hamilton, and I. Farrer, Phys. Rev. Lett. **121**, 077701 (2018).

[43] H. Liu, E. Marcellina, A. R. Hamilton, and D. Culcer, Phys. Rev. Lett. **121**, 087701 (2018).

[44] E. Marcellina, P. Bhalla, A. R. Hamilton, and D. Culcer, Phys. Rev. B **101**, 121302(R) (2020).

[45] Z. Wang, E. Marcellina, A. Hamilton, J. H. Cullen, S. Rogge, J. Salfi, D. Culcer *et al.*, npj Quantum Inf. **7**, 1 (2021).

[46] J. H. Cullen, P. Bhalla, E. Marcellina, A. R. Hamilton, and D. Culcer, Phys. Rev. Lett. **126**, 256601 (2021).

[47] N. W. Hendrickx, D. P. Franke, A. Sammak, M. Kouwenhoven, D. Sabbagh, L. Yeoh, R. Li, M. L. V. Tagliaferri, M. Virgilio, G. Capellini *et al.*, Nat. Commun. **9**, 2835 (2018).

[48] P. Philippopoulos, S. Chesi, D. Culcer, and W. A. Coish, Phys. Rev. B **102**, 075310 (2020).

[49] F. Nichele, A. N. Pal, R. Winkler, C. Gerl, W. Wegscheider, T. Ihn, and K. Ensslin, Phys. Rev. B **89**, 081306 (2014).

[50] J. Salfi, J. A. Mol, D. Culcer, and S. Rogge, Phys. Rev. Lett. **116**, 246801 (2016).

[51] M. Brauns, J. Ridderbos, A. Li, E. P. A. M. Bakkers, W. G. van der Wiel, and F. A. Zwanenburg, Phys. Rev. B **94**, 041411 (2016).

[52] M. Brauns, J. Ridderbos, A. Li, W. G. van der Wiel, E. P. A. M. Bakkers, and F. A. Zwanenburg, Appl. Phys. Lett. **109**, 143113 (2016).

[53] D. Q. Wang, O. Klochan, J.-T. Hung, D. Culcer, I. Farrer, D. A. Ritchie, and A. R. Hamilton, Nano Lett. **16**, 7685 (2016).

[54] H. Watzinger, C. Kloeffel, L. Vukusic, M. D. Rossell, V. Sessi, J. Kukucka, R. Kirchschlager, E. Lausecker, A. Truhlar, M. Glaser *et al.*, Nano Lett. **16**, 6879 (2016).

[55] J. Salfi, M. Tong, S. Rogge, and D. Culcer, Nanotechnology **27**, 244001 (2016).

[56] F. Nichele, M. Kjaergaard, H. J. Suominen, R. Skolasinski, M. Wimmer, B.-M. Nguyen, A. A. Kiselev, W. Yi, M. Sokolich, M. J. Manfra *et al.*, Phys. Rev. Lett. **118**, 016801 (2017).

[57] A. Srinivasan, D. S. Miserev, K. L. Hudson, O. Klochan, K. Muraki, Y. Hirayama, D. Reuter, A. D. Wieck, O. P. Sushkov, and A. R. Hamilton, Phys. Rev. Lett. **118**, 146801 (2017).

[58] S. Conesa-Boj, A. Li, S. Koelling, M. Brauns, J. Ridderbos, T. T. Nguyen, M. A. Verheijen, P. M. Koenraad, F. A. Zwanenburg, and E. P. A. M. Bakkers, Nano Lett. **17**, 2259 (2017).

[59] S.-X. Li, Y. Li, F. Gao, G. Xu, H.-O. Li, G. Cao, M. Xiao, T. Wang, J.-J. Zhang, and G.-P. Guo, Appl. Phys. Lett. **110**, 133105 (2017).

[60] J.-T. Hung, E. Marcellina, B. Wang, A. R. Hamilton, and D. Culcer, Phys. Rev. B **95**, 195316 (2017).

[61] S. Liles, R. Li, C. H. Yang, F. E. Hudson, M. Veldhorst, A. S. Dzurak, and A. R. Hamilton, Nat. Commun. **9**, 3255 (2018).

[62] L. Vukusic, J. Kukucka, H. Watzinger, J. M. Milem, F. Schaffler, and G. Katsaros, Nano Lett. **18**, 7141 (2018).

[63] Y. Li, S.-X. Li, F. Gao, H.-O. Li, G. Xu, K. Wang, D. Liu, G. Cao, M. Xiao, T. Wang *et al.*, Nano Lett. **18**, 2091 (2018).

[64] A. Crippa, R. Maurand, L. Bourdet, D. Kotekar-Patil, A. Amisse, X. Jehl, M. Sanquer, R. Lavieville, H. Bohuslavskyi, L. Hutin *et al.*, Phys. Rev. Lett. **120**, 137702 (2018).

[65] N. W. Hendrickx, W. I. L. Lawrie, L. Petit, A. Sammak, G. Scappucci, and M. Veldhorst, Nat. Commun. **11**, 3478 (2020).

[66] D. S. Miserev, A. Srinivasan, O. A. Tkachenko, V. A. Tkachenko, I. Farrer, D. A. Ritchie, A. R. Hamilton, and O. P. Sushkov, Phys. Rev. Lett. **119**, 116803 (2017).

[67] R. Moriya, K. Sawano, Y. Hoshi, S. Masubuchi, Y. Shiraki, A. Wild, C. Neumann, G. Abstreiter, D. Bougeard, T. Koga *et al.*, Phys. Rev. Lett. **113**, 086601 (2014).

[68] E. Rashba and E. Y. Sherman, Phys. Lett. A **129**, 175 (1988).

[69] See Supplemental Material at http://link.aps.org/supplemental/10.1103/PhysRevB.107.L041301 for additional details of the calculation.

[70] D. Culcer, A. Sekine, and A. H. MacDonald, Phys. Rev. B **96**, 035106 (2017).

[71] Y. Ohno, D. Young, B. a. Beschoten, F. Matsukura, H. Ohno, and D. Awschalom, Nature **402**, 790 (1999).

[72] H. Ohno, D. Chiba, F. Matsukura, T. Omiya, E. Abe, T. Dietl, Y. Ohno, and K. Ohtani, Nature **408**, 944 (2000).

[73] T. Fukumura, T. Shono, K. Inaba, T. Hasegawa, H. Koinuma, F. Matsukura, and H. Ohno, Phys. E **10**, 135 (2001).

[74] H. Tang, S. Masmanidis, R. Kawakami, D. Awschalom, and M. Roukes, Nature **431**, 52 (2004).

[75] C. Gould, C. Rüster, T. Jungwirth, E. Girgis, G. M. Schott, R. Giraud, K. Brunner, G. Schmidt, and L. W. Molenkamp, Phys. Rev. Lett. **93**, 117203 (2004).

[76] C. Rüster, T. Borzenko, C. Gould, G. Schmidt, L. W. Molenkamp, X. Liu, T. J. Wojtowicz, J. K. Furdyna, Z. G. Yu, and M. E. Flatté, Phys. Rev. Lett. **91**, 216602 (2003).

[77] A. D. Giddings, M. N. Khalid, T. Jungwirth, J. Wunderlich, S. Yasin, R. P. Campion, K. W. Edmonds, J. Sinova, K. Ito, K. Y. Wang, D. Williams, B. L. Gallagher, and C. T. Foxon, Phys. Rev. Lett. **94**, 127202 (2005).

[78] I. Krainov, V. Sapega, G. Dimitriev, and N. Averkiev, J. Phys.: Condens. Matter **33**, 445802 (2021).

[79] S. Lee, J.-H. Chung, X. Liu, J. K. Furdyna, and B. J. Kirby, Mater. Today **12**, 14 (2009).